Vivek G. Trivedi[1]
Kirti Mangliya[2]
Vimal R. Patel[3]
Mazar A. Shaikh[4]
Shyam K. Dabhi[5]
Dipakkumar J. Parmar[6]
Saurabh P. Shah[7]

Optimizing Indirect Liquid Cooling System for Thermal Management of Electric Vehicle Battery: A CFD Study Using Cold Plate

JES Journal of Electrical Systems

Abstract: - Traditional fuels and internal combustion engines are major sources of CO2 emissions and environmental pollution. Electric vehicles (EVs) are touted as green energy solutions for a cleaner future. EVs utilize lithium-ion batteries, but face challenges such as poor performance in extreme temperatures, limited electrode lifespan, and safety risks from battery thermal runaway. Effective Battery Thermal Management Systems (BTMS) are crucial for EV longevity. The study emphasizes the crucial role of coolant selection, structural design, and channel configuration in optimizing indirect liquid cooling systems for EV batteries. Conducted through comprehensive CFD analysis using a cold plate, it specifically examined three key parameters: the impact of different coolants, various cold plate structures, and the number of channels. Findings indicated that a 50% ethylene glycol-water (EGW) solution outperformed pure water in performance metrics. Additionally, streamlined channel cold plates demonstrated superior temperature uniformity and reduced pressure drops, establishing them as the most efficient design option. This streamlined design facilitated enhanced heat transfer while minimizing pressure losses, confirming its suitability for EV battery cooling applications.

Keywords: Electric vehicle, Battery thermal management system, Indirect liquid cooling, Cold plate, CFD simulations, Heat transfer

Nomenclature

LIB	Lithium-ion Battery
BTMS	Battery Thermal management system
PCM	Phase change material
CFD	Computational fluid dynamics
GPM	Grams per minute
D	Width of the main channel (mm)
Tmax	Maximum temperature (°C)
ΔTavg	Average temperature (°C)
Δp	Pressure drop (pa)
PMCP	Parallel mini-channel cold plate
BLC	Bottom liquid cooling
EGW	Ethylene glycol water solution
PGW	Propylene glycol water solution

1. Introduction

As the energy crisis and environmental pollution become prominent, the vigorous development of clean energy, the improvement of the surroundings and the promotion of green and occasional CO2 production have end up a vital mission. Traditional fuel vehicles run mainly on non-renewable fossil energy, which not only consumes

[1] [1*,2,7]Mechanical Engineering Department, L.D. College of Engineering, Gujarat Technological University, Ahmedabad, Gujarat 380 015, India

[3,4]Automobile Engineering Department, L.D. College of Engineering, Gujarat Technological University, Ahmedabad, Gujarat 380 015, India

[5]Mechanical Engineering Department, Government Engineering College, Palanpur, Gujarat-385001, Gujarat Technological University, India

[6]Mechanical Engineering Department, Government Engineering College, Patan, Gujarat-384265, Gujarat Technological University, India

*** Corresponding author:** Vivek G. Trivedi

*E-mail addresses: vivekgtrivedi@gmail.com, vgtrivedi@ldce.ac.in

more fossil energy, but also produces emissions that contribute to the greenhouse effect. In this context, electric vehicles have attracted much attention due to their benefits including low pollution and high performance [1]. A primary assignment in improvement of electrical automobiles is to discover a appropriate electricity storage system that allows battery automobiles to drive for a long time and accelerate quickly. The ideal energy storage solution for electric vehicles is characterized by high specific energy and capacity, low self-discharge rates, high voltage, extended service life, and efficient recyclability [2]. However, the performance of lithium-ion batteries is significantly influenced by operating and storage temperatures.

Typically, the optimal temperature range for lithium-ion batteries lies between 15°C and 40°C, with a recommended maximum temperature difference of 5°C between the batteries and the ambient environment [3].

The maximum temperature difference is the maximum difference value stored in the battery. High temperatures increase the reaction rate resulting in higher power and output but at the same time cause even higher temperatures and increased heat load [4]. If the heat is not dissipated at least as fast as it is generated in the batteries, temperatures can rise uncontrollably resulting in the deterioration of parts and materials or possibly the batteries' thermal runaway. Thermal runaway puts the safety of the car and its occupants at jeopardy since it can cause a fast rise in temperature, the development of gases, or even a battery explosion. [5]. Therefore, a reasonable and efficient battery thermal management system (BTMS) is necessary for the safe operation of the battery module and good charging and discharging performance. The two primary ways that a battery cell produces heat are through electrochemical reaction and joule heating, which is brought on by the flow of electrons inside the battery cells [6]. The optimal operating temperature range for lithium-ion batteries is between 15°C and 40°C; temperatures higher than 50°C might be detrimental to the batteries' lifespan. The performance and efficiency of the entire battery might be considerably lowered by the premature wear of even one cell. The primary goal of BTMS is to control battery cell temperature in order to prolong battery life. Heat pipes, composite cooling, phase change material (PCM), air cooling, and liquid cooling are the several types of popular BTMSs now on the market.

2. Methodology

This chapter presents the selected research strategy and method used to answer the research question. Three different cooling plate were studied in this thesis. The objective for the three different cooling plate was to find optimum plate by simulation using Ansys Fluent.

2.1 Configuration of liquid cooling system

The lithium-ion battery's heat created during the charging or discharging process is eliminated by the liquid cold plate, an essential component of a liquid cooling system for battery thermal functioning. It is well established that the thermal properties of a lithium-ion battery have a significant relationship with the battery's ability to charge and discharge. This is especially true when it comes to the cooling capacity of a liquid cold plate. In order to keep the battery temperature within a suitable and safe range, the BTMS relies heavily on the creation of a liquid cold plate with great efficiency.

It is evident from this that further research on liquid cold plates is required in order to determine the ideal operating parameters for lithium-ion battery cooling. Using CREO software, a three-dimensional model was initially created for the above-mentioned reasons. Lithium-ion battery heat generation under discharge rate was handled as a surface heat source in order to simplify the model. The study's goals were to determine the maximum temperature differential and average temperature on the liquid cold plate, which were used to assess the thermal state of the lithium-ion battery module. The dimensions of the battery are 220 mm (x), 135 mm (y), and 30 mm (z), and its characteristics are displayed in Table 1. The cold plate is arranged on the side surface of the battery module, as displayed in Figure 1. The length, width, and thickness of the cold plate are 220 mm, 135 mm, and 8 mm, respectively.

Figure 1. Schematic diagram of lithium-ion battery module.

In this study first the performance of different coolants is analyzed and then three different plates. The three plates used in this study are straight plate which is shown in Figure 2, serpentine plate which is shown in Figure 3 and streamline channel plates which are shown in Figure 4. Based on the initial simulation results, streamline plate is further analyzed using various parameters that affects the liquid cooling. Initially the liquid cold is having 4 channels of 5 mm width, further number of channels are changed to analyzed the performance of the cold plate.

Table 1. Battery Specifications [7].

Anode material	LiFePO4
Cathode material	Graphite
Electrolyte	LiPF6
Hardness (HV0.2)	300
Geometric parameter (mm)	220×30×135
Nominal capacity (Ah)	60
Nominal voltage (V)	3.2
Maximum charging voltage (V)	3.6
Discharge cut-off Voltage (V)	2.5
Charge cut-off voltage (V)	3.65
Maximum charging current (C)	1 Ca)
Maximum discharging current (C)	5 Ca) (20 s)
Standard charging current (C)	1/3 Ca)
Quick charging current (C)	1 Ca)
Internal resistant (mΩ)	≤1
Normal charging temperature (°C)	0–45
Normal discharge temperature (°C)	20–55
Storage temperature (1 month) (°C)	–20–45

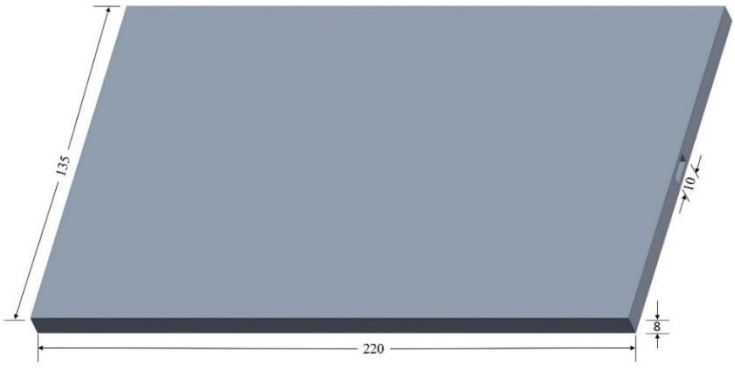

(a)

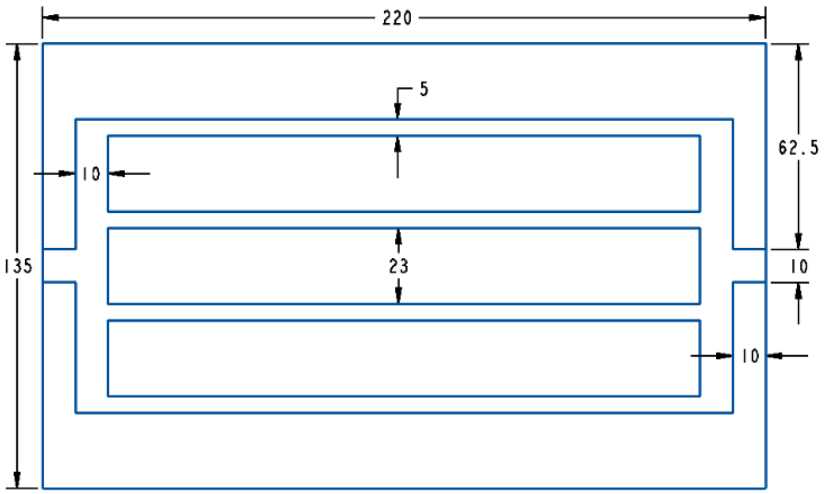

(b)

Figure 2. Straight plate. (a) Cad model. (b) 2D drawing

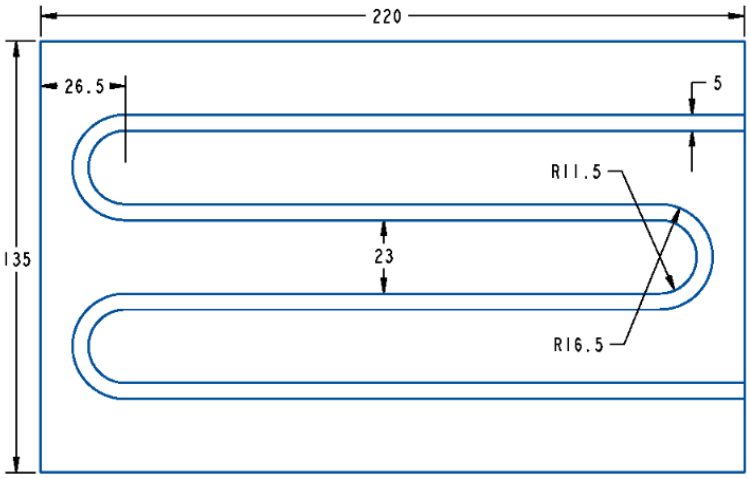

Figure 3. Serpentine plate.

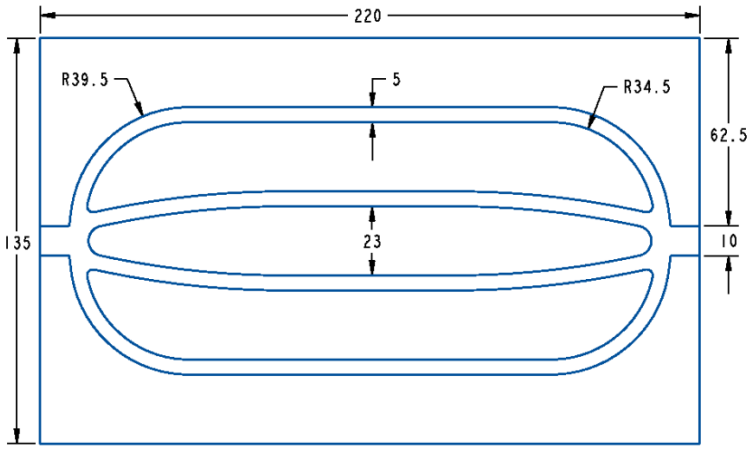

(a)

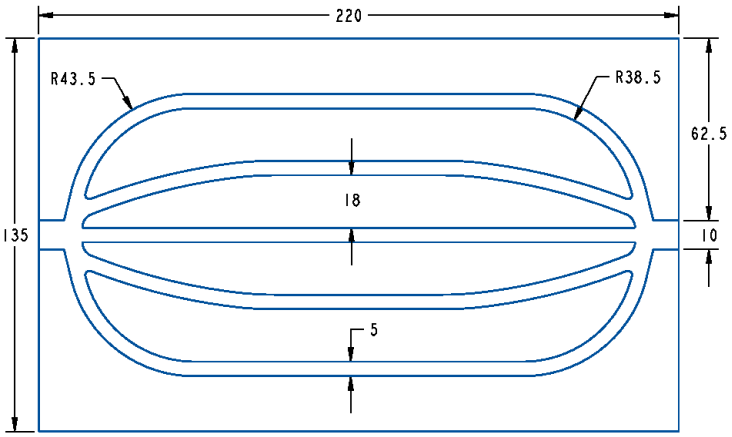

(b)

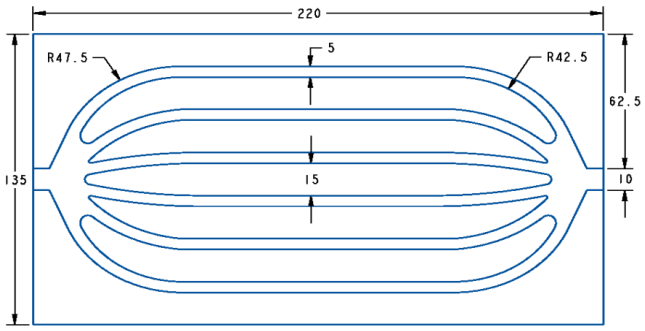

(c)

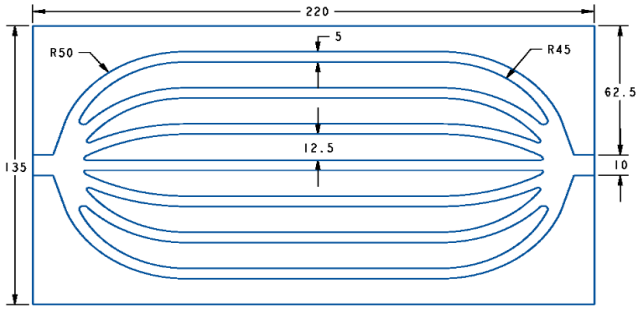

(d)

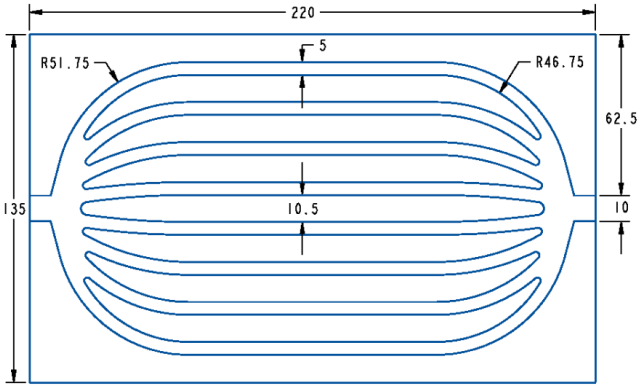

(e)

Figure 4. Streamline plate. (a) 4 channels. (b) 5 channels. (c) 6 channels. (d) 7 channels. (e) 8 channels.

2.2. Parameters of liquid cooling

Liquid cooling is a highly effective thermal management approach that can regulate the battery's temperature and temperature differential within a reasonable range. The various factors such as coolant, flow channel optimization and structure optimization directly affect the heat dissipation of the battery by indirect cooling method. Coolant selection, especially considering viscosity, density, thermal conductivity, specific heat capacity, and flow rate, significantly impacts cooling efficiency. Water emerges as a widely used coolant due to its high thermal conductivity, low viscosity, and superior heat transfer capabilities compared to air or oil. Water/glycol mixtures expand the operational range of battery thermal management systems (BTMSs) and minimize potential battery damage from water condensation. Balancing coolant flow rates becomes crucial for effective heat dissipation without excessive energy consumption. Studies highlight the importance of finding the optimal flow rate to achieve efficient cooling without increasing the pump's power consumption unnecessarily [8,9]. Researchers investigate various channel geometries for cold plates, including multichannel parallel, serpentine, streamlined, U-shaped, snake, and hexagonal structures. Studies analyze the effects of these designs on coolant flow resistance and battery temperature distribution. They reveal insights into which designs offer improved cooling efficiency and pressure drop variations, crucial factors in BTMS design [10,11,12]. Moreover, investigations focus on channel parameters like width, spacing, and the integration of micro channels.

These studies underscore how adjusting channel dimensions can optimize cooling efficiency by minimizing pressure drops and increasing heat transfer area and thermal conductivity through micro channel integration. Structural optimization within indirect liquid cooling systems for batteries, focusing on factors such as cold plate location, contact area with the battery, number of cooling channels, flow rate, and their influence on cooling efficiency and energy consumption [13]. The number and direction of cooling channels significantly affect cooling efficiency. Optimal channel numbers exist to prevent uneven flow rates and temperature variations among cells. Additionally, the flow direction's impact on cooling efficiency depends on the coolant flow rate. The various selected parameters for this research are shown in Table 2.

Table 2. Selected parameters.

Coolant	Water	25% ethylene glycol aqueous solution	50% ethylene glycol aqueous solution	25% propylene glycol aqueous solution	50% propylene glycol aqueous solution
Type of channel	Straight	Serpentine	Streamline	-	-
No of Channels	4	5	6	7	8

The above parameters are selected by studying the various research paper mentioned in chapter two. The various parameters such as coolant is vital for the efficient cooling of the system. The structure of the cold plate also highly influences the performance. Then other parameters such as channel width and number also effect the performance of the system. The mass flow rate decreases the overall temperature but increases the pressure drop of the system. The inlet temperature of the coolant also significantly lowers the temperature. Thermal properties of the various coolant medium and aluminum cold plate are shown in Table 3.

Table 3. Thermal properties of the medium and plate.

Coolant	**Dynamic viscosity (pa·s)**	**Conductivity (w·m−1·K−1)**	**Specific heat (j·kg−1·K−1)**	**Density (kg·m−3)**
Water	0.000833	0.606	4179	996.31
25% ethylene glycol aqueous solution	0.002855	0.279	3850	1060
50% ethylene glycol aqueous solution	0.003982	0.384	3300	1071.11

25% propylene glycol aqueous solution	0.002852	0.277	3780	1060.1
50% propylene glycol aqueous solution	0.003671	0.282	3640	1070
Cold plate	-	202.4	871	2719

2.3. Analytical equations and boundary conditions.

The heat generated by the cell is convected by the liquid, which is obtained as follows;

$$Q=Ah\,(T_{cell}-T_{fluid}) \quad (1)$$

where A represents the cell's area, h stands for the heat transfer coefficient, Tcell denotes the battery cell's temperature, Tfluid denotes the coolant's temperature, and the fluid's overall temperature rise is calculated using

$$Q=\dot{m}Cp\,(T_{out\ flow}-T_{in\ flow}) \quad (2)$$

where the specific heat capacity is represented by Cp and the mass flow rate by $\dot{m}$. What determines the kind of flow is its Reynolds number, which is:

$$Re=\frac{\rho vD}{\eta} \quad (3)$$

where D is the hydraulic diameter (i.e., 3.33 mm) of the rectangular channel, v is the velocity, and ρ is the water density. The mass flow rate was fixed at 0.004 kg/s for this investigation. Laminar flow (Re < 2000) is represented by the appropriate Reynolds number of 80. The analytical model should choose the laminar model. The cold plate's internal channel's pressure drop is

$$\Delta p=\frac{v^2 fl\rho}{2D} \quad (4)$$

where D is the hydraulic diameter, l is the channel flow length, f is the friction factor, and v is the fluid velocity. For the friction factor, the formula is

$$f=F\frac{64}{Re} \quad (5)$$

where F, the form factor, is 0.89 in the case of non-circular ducts. The equations controlling the conservation of mass, momentum, and energy in a Newtonian incompressible fluid are solved in this article using Ansys Fluent, and the transient state is also solved. The SIMPLE algorithm with second- and third-order equations was used to combine the continuity and momentum equations. Only the transient state is considered in this study, and the relevant equations are presented below. The equations for conservation of mass, conservation of momentum and conservation of energy for the cooling and heating are;

Continuity equation $\frac{\partial\rho}{\partial t}+\nabla\cdot(\rho u)=0$ (6)

X-momentum $\frac{\partial(\rho u)}{\partial t}+\nabla\cdot(\rho uu)=-\frac{\partial P}{\partial x}+\nabla\cdot(\mu\nabla u)+SMx$ (7)

Y-momentum $\frac{\partial(\rho v)}{\partial t}+\nabla\cdot(\rho vu)=-\frac{\partial P}{\partial y}+\nabla\cdot(\mu\nabla v)+SMy$ (8)

Z-momentum $\frac{\partial(\rho w)}{\partial t}+\nabla\cdot(\rho wu)=-\frac{\partial t}{\partial z}+\nabla\cdot(\mu\nabla w)+SMw$ (9)

Energy equation $mCp\frac{dTc}{dt}=\nabla\cdot(\lambda c\nabla Tc)+Qg$ (10)

where ρ indicates the density of the medium ($kg\cdot m^{-3}$), u,v and w are the flow rate of the medium ($m\cdot s^{-1}$), μ indicates the dynamic viscosity of the medium (Pa·s), cp is the heat capacity of the medium ($J\cdot kg^{-1}K^{-1}$).

In the heat generation model, the internal resistance of the battery was assumed to be constant at ambient temperature. According to the classic model proposed by Bernardo, the heating capacity of batteries was

determined in the equation below. The model did not take into account the heat from polarization, chemical reactions, or electrode coating.

$$q = \frac{I}{V}\left[(U0 - U) - \frac{\partial U0}{\partial T}\right] \quad 11$$

The battery volume, V, is measured in cubic meters; the open circuit voltage, U, and operating voltage, T, are measured in volts; the temperature, T, is expressed in Kelvin. At room temperature and low discharge, the values of "∂U0" and "∂T" are negligible and can be disregarded. Equation (11) can therefore be reduced and written as follows:

$$q = \frac{I}{V}(U298.15 - U) = \frac{I^2(RP + Re)}{V} = \frac{I^2R}{V} \quad 12$$

U298.15, which is the battery's open circuit voltage at 298.15 K in volts, and R, which is the total internal resistance in ohms derived from the internal resistance Re and the internal resistance Rp associated with polarization, serve as indicators. Different parts of the battery, such as the positive and negative electrodes, the connection, and the welding position of the conductor, generate heat in addition to the complex heat production inside the battery. You can overlook these heats when researching battery heat generation. To calculate the battery's thermal capacity in this investigation, utilize Equation (12). For a lithium battery discharge rate of 0.6 C, the heat generation rate was 1454.5454 W/m^3. Measured in relation to its rated capacity, the C-rate represents the charge and discharge current. The boundary conditions used for the analysis are shown in Table 4 and Figure 5.

Table 4. Boundary conditions.

Boundary Conditions	**Value**	**Units**
Heat flux	1454.5454	W/m^3
Mass flow inlet	0.004	Kg/s
Pressure outlet	0	Pa
Convective HTC of air	3.9	W/m^2 -k

First from the above equation first the heat flux is calculated. After that all the boundary conditions are applied at inlet and outlet of the cooling plate. This boundary conditions are same as used in experimental procedure. Same boundary conditions are necessary to kept to validate the simulation and experimental pressure.

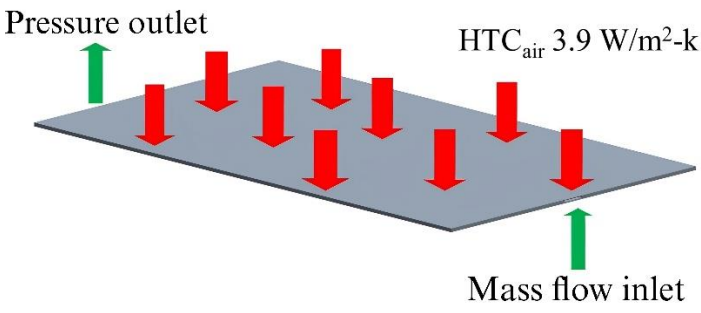

Figure 5. Boundary conditions.

For meshing of the cold plate polyhedral mesh is used, which is shown in Figure 6. For verification of the grid independence on maximum temperature and pressure drop, various grid sizes are selected to check the model. The result of the grid independence study is shown in Figure 7. In this study at 0.5 mm mesh size the maximum temperature and pressure drop are stable with grid no of 4629904. Thus, for all other plates in this study mesh size of 0.5 mm is used.

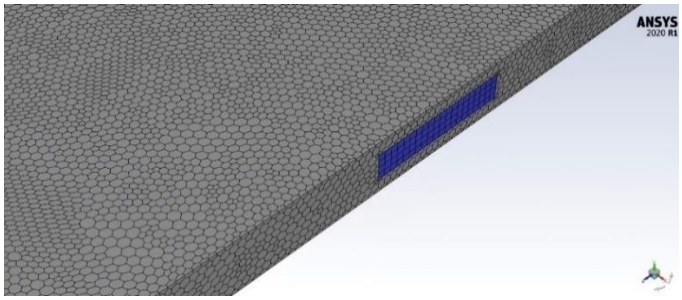

Figure 6. Meshed model.

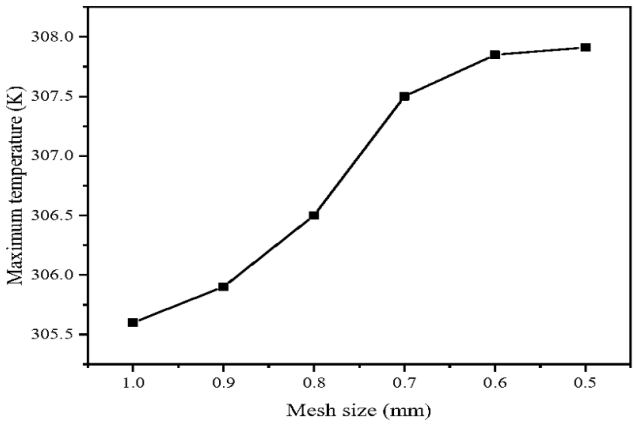

(a)

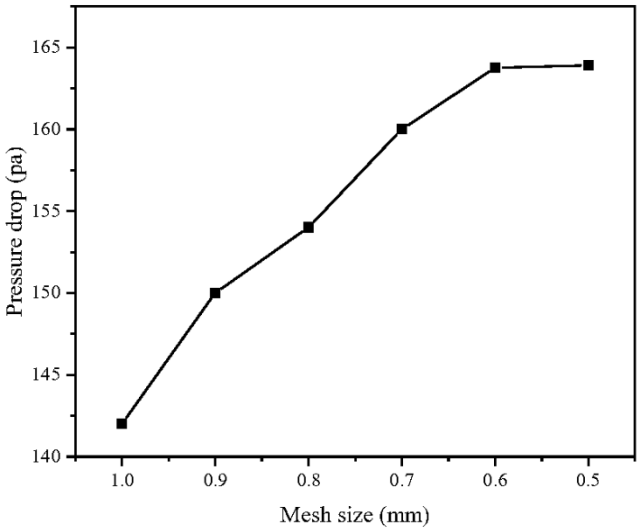

(b)

Figure 7. Mesh convergence study. (a) Maximum temperature. (b) Pressure drops.

3. Results and discussion

This study looked into a cold plate's cooling effectiveness. In the initial study, the channel's width was fixed at 5 mm. As seen in Table 4, additional boundary conditions were implemented and air was defined around the cold plate. In order to verify and assess the dependability of the results obtained, critical parameters such as maximum temperature, and temperature differential were tracked and compared with the findings of XU et al. [13] during the solution process.

3.1. Validation

For the numerical validation XU et. al. [13] study was chosen to compare the simulation results with experimental results. In his study the battery used was life po4 prismatic cell lithium-ion battery. The discharge rate for comparing the results is selected as 0.6 C from his study. The other boundary conditions are mentioned in Table 4. The maximum temperature of the battery in experimental study is recorded as 35 °C. Throughout the solving process, the crucial parameters, such as the temperature differential, maximum temperature, and flow pressure drop were kept an eye on. The straight channel cold plate's temperature and pressure distribution are displayed in Figure 8 and comparison between simulation and experimental result is shown in Figure 9.

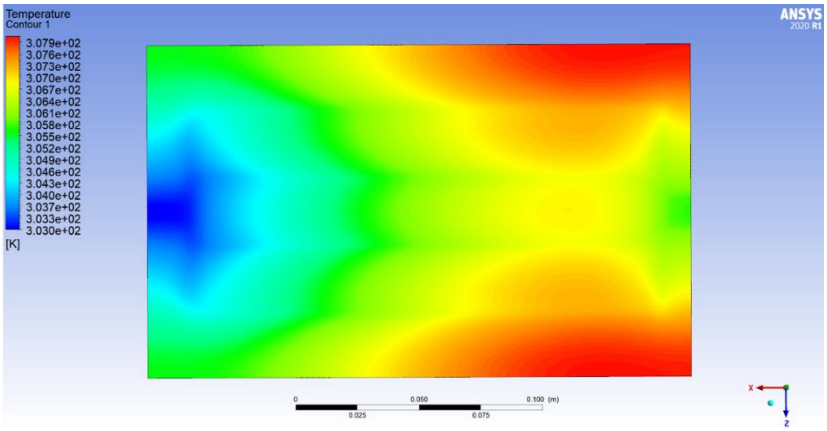

(a)

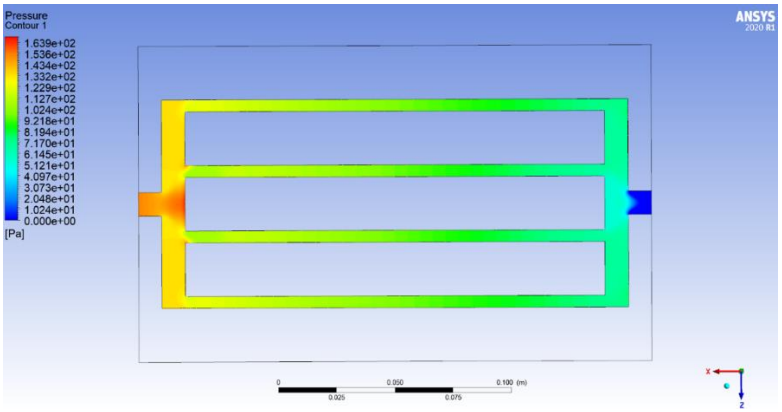

(b)

Figure 8. Straight channel cold plate. (a) Temperature distribution. (b) Pressure distribution.

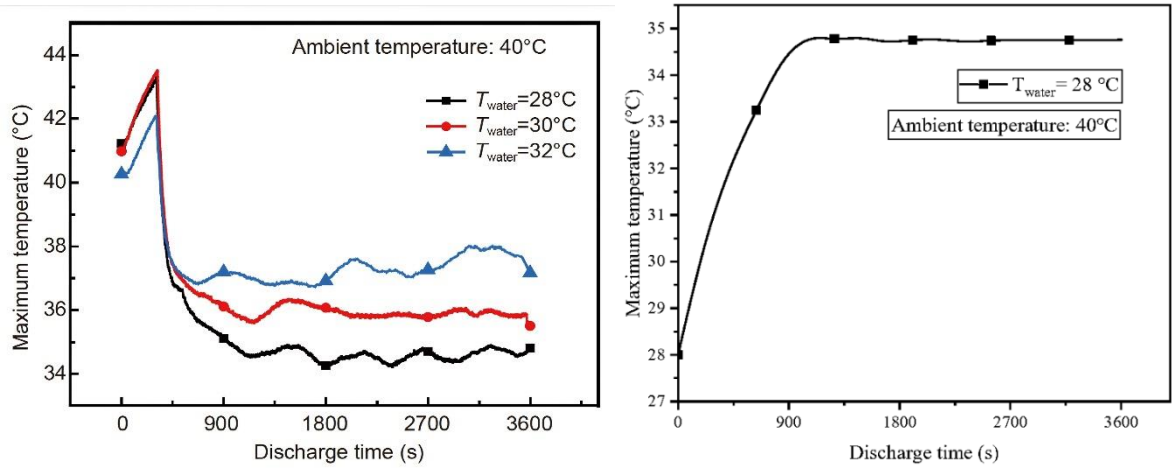

(a) (b)

Figure 9. Maximum temperature. (a) Simulation result. (b) Experimental result. [10]

According to simulation result, the cold plate's maximum surface temperature is 307.91 K (34.76 °C) and min. temp. is 303 K (29.85 °C), there is a 163.9 pa pressure drop, and there is a maximum temperature differential of 4.91 K. The study's experimental temperature is 35 °C. Thus, the percentage error in the simulation is about 0.69%. We can conclude from the simulation results that there is a comparable outcome between the simulation and experimental outcomes. Thus, a degree of confidence in the validity and accuracy of findings is established by contrasting simulation results with the results of the current experimental study. The validation procedure strengthened the validity of the result by confirming that the simulation methods and underlying assumptions are in line with accepted literature.

3.2. Effect of different coolants

In this section the effect of different coolants is analyzed on the cold plate. The different coolant and their properties are mentioned in Table 3. Ethylene glycol and propylene glycol are generally added in the coolant to increase the freezing point of the coolant. The temperature and pressure distribution for 25% EGW is shown in Figure 10, for 50% EGW it is shown in Figure 11, for 25% PGW it is shown in Figure 12, and for 50% PGW it is shown in Figure 13. The temperature and pressure distribution for the same is shown in Figure 14 and the comparison between coolants is shown in Table 5.

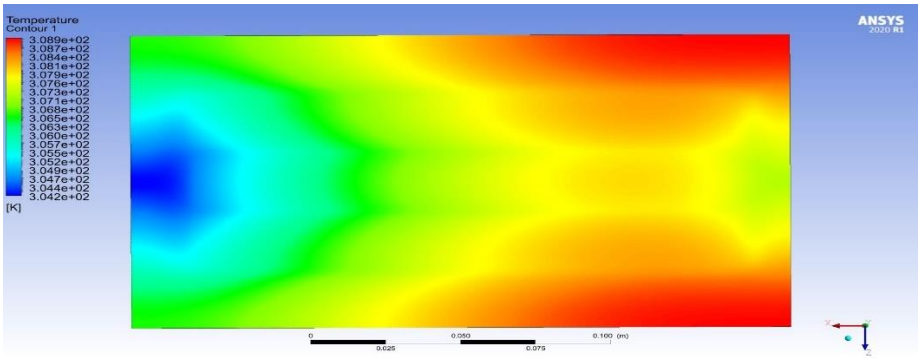

(a)

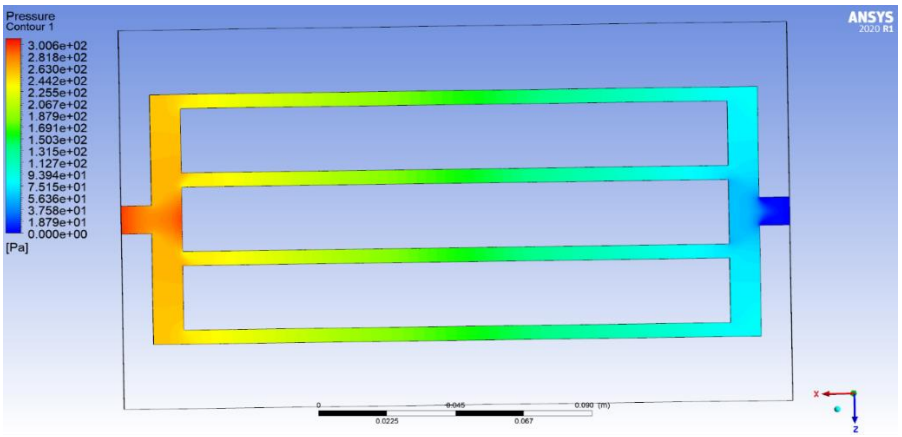

(b)

Figure 10. 25% EGW. (a) Temperature distribution. (b) Pressure distribution.

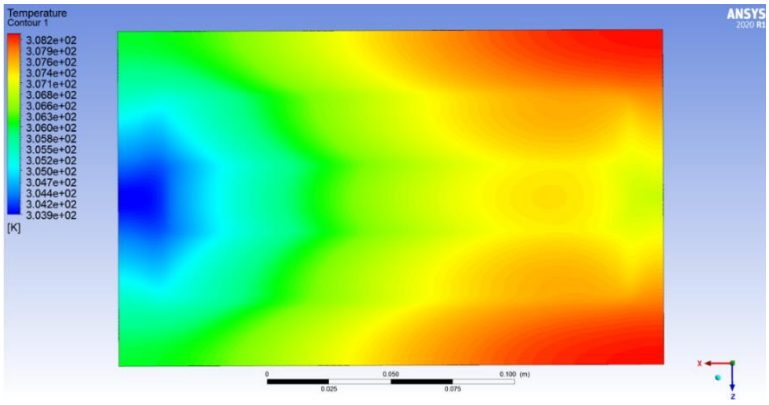

(a)

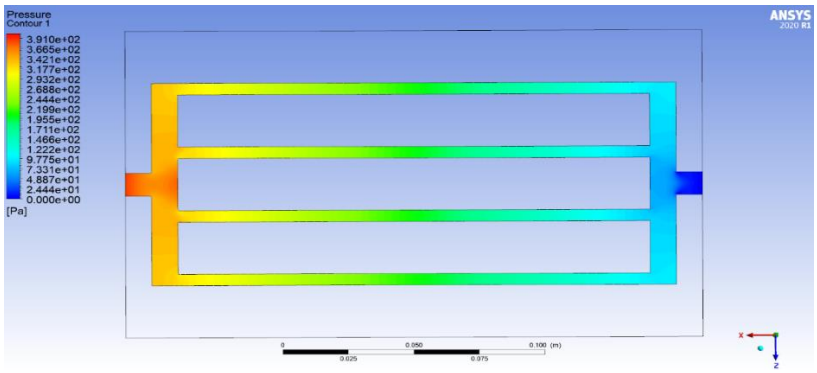

(b)

Figure 11. 50 % EGW. (a) Temperature distribution. (b) Pressure distribution.

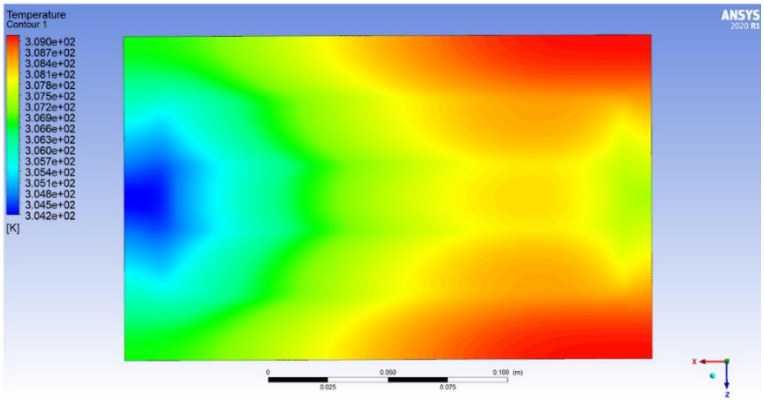

(a)

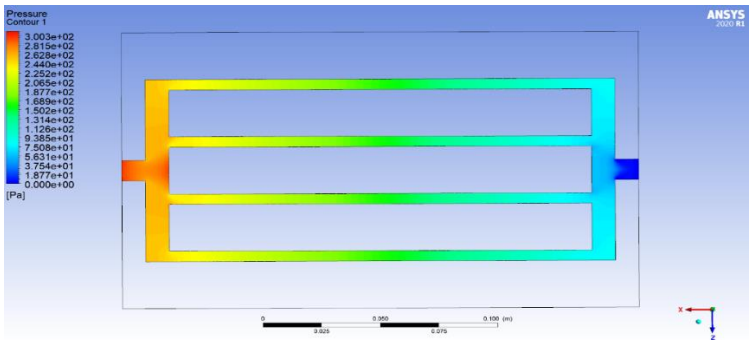

(b)

Figure 12. 25% PGW. (a) Temperature distribution. (b) Pressure distribution.

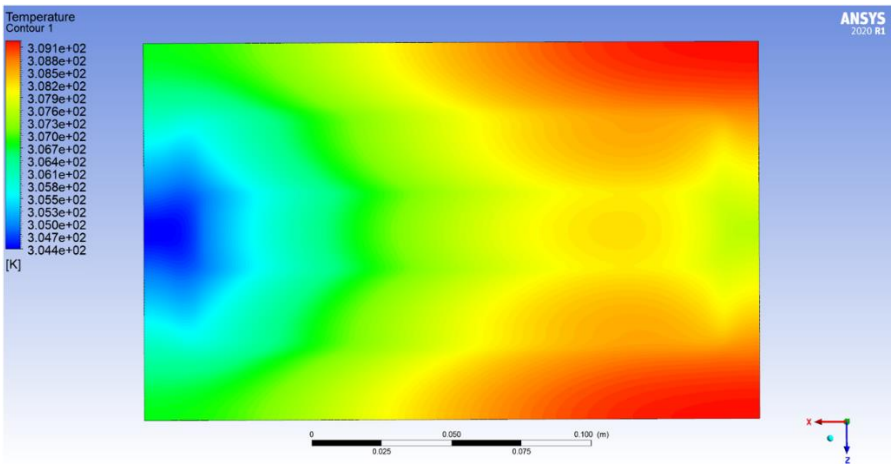

(a)

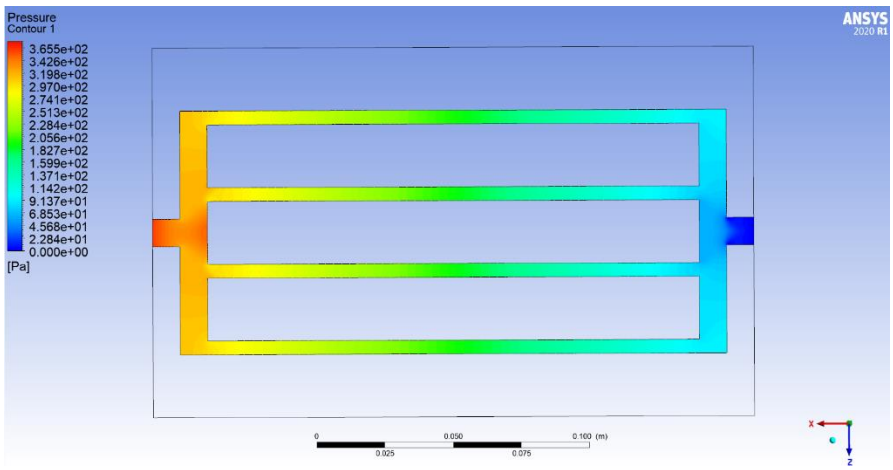

(b)

Figure 13. 50 % PGW. (a) Temperature distribution. (b) Pressure distribution.

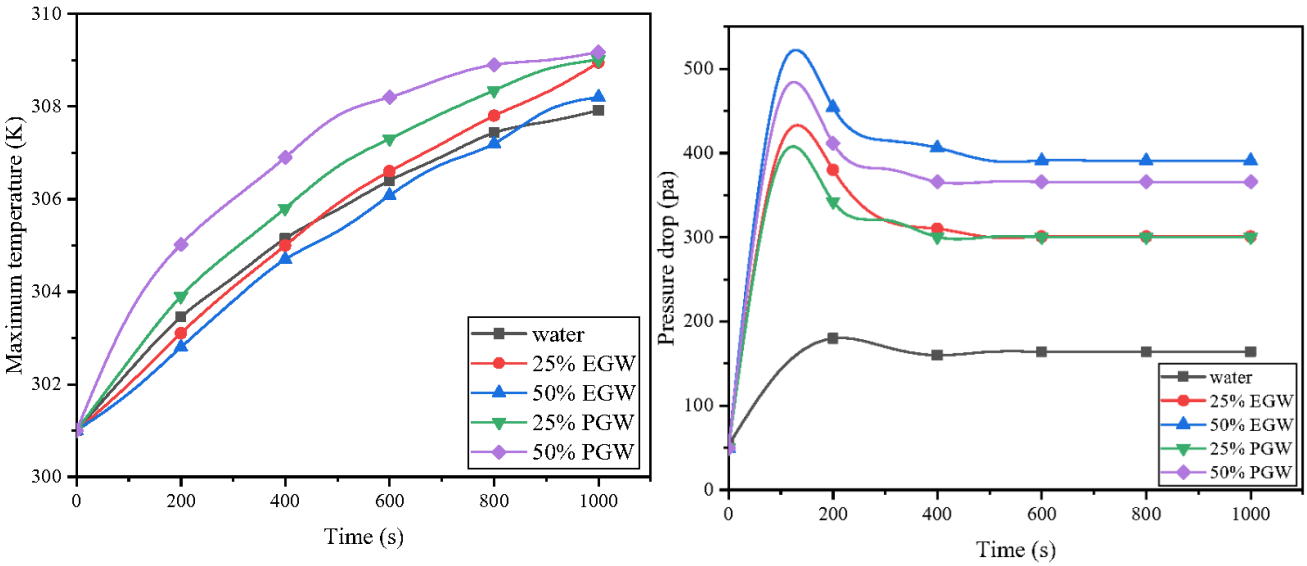

(a) (b)

Figure 14. Different coolants. (a) Temperature gradient. (b) Pressure gradient.

Table 5. Comparison of different coolants.

Coolant	Max. Temperature (K)	Max. Temperature Difference (K)	Pressure Drop (Pa)
Water	307.91	4.91	163.9
25 % EGW	308.94	4.75	300.6
50 % EGW	308.2	4.21	391
25 % PGW	309.01	4.81	300.32
50 % PGW	309.17	4.77	365.583

When water is used maximum surface temperature is 307.91 K (34.76 °C), the pressure drop is 163.9 pa. and the maximum temperature difference is 4.91 K. By comparing these results, we can say that the lowest surface temperature is achieved when water is used and the temperature difference achieved in this solution is high compared to other coolants. The maximum temperature difference indicates the temperature uniformity of the cold plate, the lower temperature difference means better performance. The Ethylene glycol solution is generally used to reduce freezing point temperature and improve corrosion resistance. It also raises the boiling point temperature that is important for the hot day conditions when the higher temperature difference between air and coolant is desirable as it improves the heat transfer performance of the cooling plate. Thus, for further analysis the 50 % EGW solution is used.

3.3. Effect of different structure

In this section serpentine channel and streamline channel cold plate is analyzed and their results are compared with the straight channel cold plate which is shown in Table 6. The coolant used is 50 % EGW solution. Temperature and pressure distribution for serpentine is shown in Figure 15 and in Figure 16 for streamline. The temperature and pressure gradient for same is shown in Figure 17.

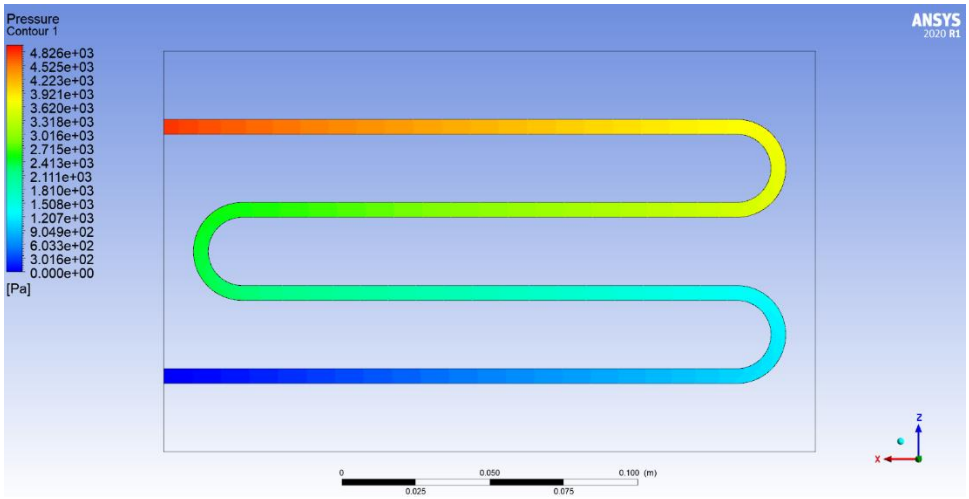

(a)

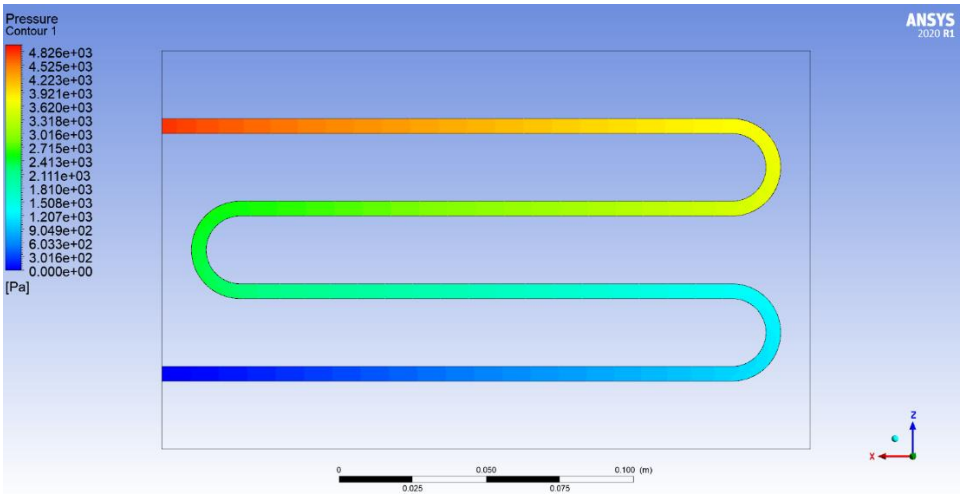

(b)

Figure 15. Serpentine channel cold plate. (a) Temperature distribution. (b) Pressure distribution.

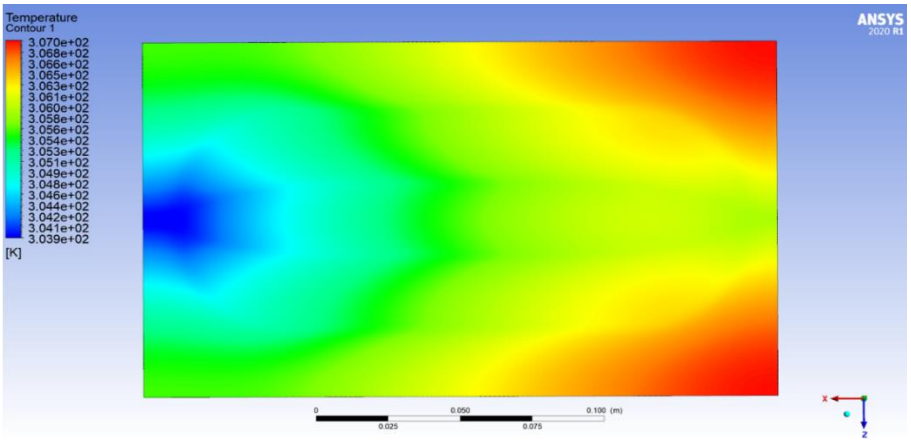

(a)

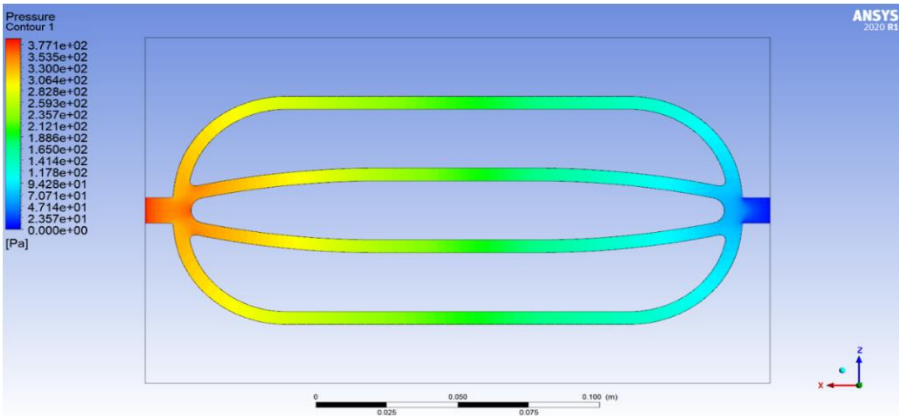

(b)

Figure 16. Streamline channel cold plate. (a) Temperature distribution. (b) Pressure distribution.

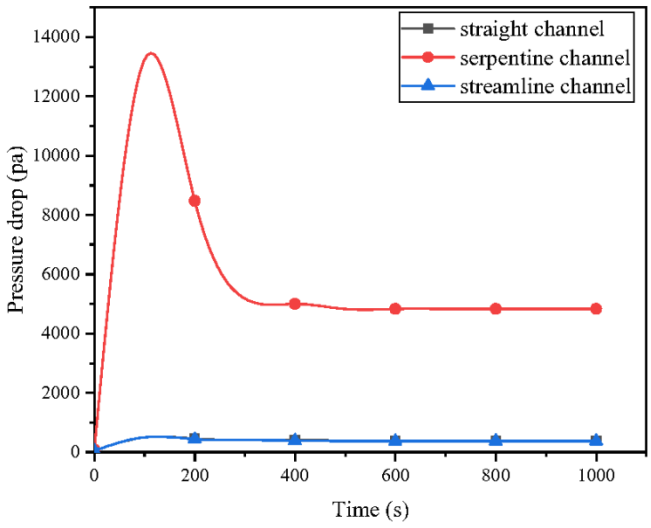

(a)

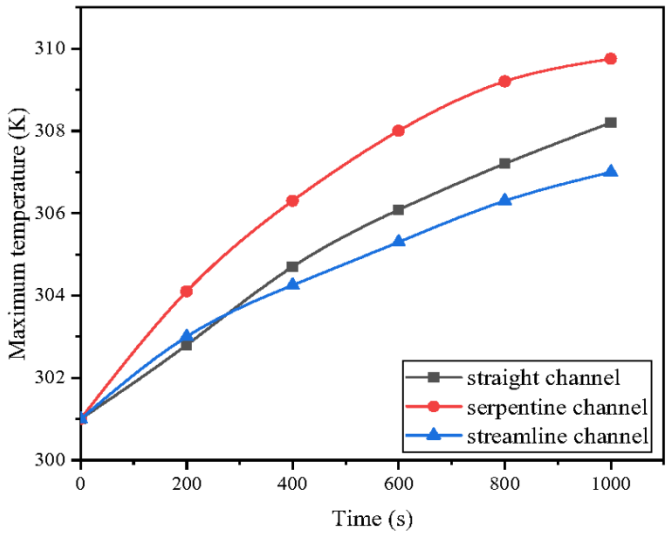

(b)

Figure 17. Different plates. (a) Temperature gradient. (b) Pressure gradient.

Table 6. Comparison of different plate structure.

Plate	**Max. Temperature (K)**	**Max. Temperature Difference (K)**	**Pressure Drop (Pa)**
Straight channel	308.2	4.21	391
Serpentine channel	309.75	4.62	4826.42
Streamline channel	307	3.15	377.16

There is a maximum temperature differential of 4.62 K, a maximum temperature of 309.75 K, and a pressure drop of 4826.42 pa in serpentine plate. The streamline channel cold plate's maximum temperature, maximum temperature differential, and pressure drop are displayed in the Figure 16. The maximum temperature is 307, maximum temperature difference is 3.15 K and the pressure drop is 377.16 pa. While in the straight channel cold plate maximum surface temperature is 308.2 K, the pressure drop is 391 Pa. and the maximum temperature

difference is 4.21 K. From the above results it is concluded that the streamline channel cold plate has minimum maximum temperature, maximum temperature difference and pressure drop. The pressure drop is reduced 92.17% from serpentine to streamline plate and maximum temperature is slightly less in streamline channel cold plate and the pressure drop in serpentine channel cold plate is drastically increase. The temperature of the streamline channel is approximately 3.42% less than the temperature of the straight channel. The temperature of the serpentine channel is approximately 4.42% more than the temperature of the straight channel. The pressure drop of the streamline channel is approximately 3.54% less than the pressure drops of the straight channel. Thus, results for further analysis streamline channel cold plate are used.

3.4. Effect of number of channels

Four further models were created in order to examine the impact of various channels on the cold plate. At 4 g/s, the coolant's mass flow rate was adjusted. At 301.15 K, the environment and coolant temperatures were set. The coolant flows outward in a rightward direction in the temperature distribution represented below. In this section different channel numbers such as 5,6,7, and 8 are analyzed. Temperature and pressure distribution for 5 channels is shown in Figure 18, for 6 channels in Figure 19, for 7 channels in Figure 20 and for 8 channels in Figure 21. The temperature and pressure gradient for same is shown in Figure 22. Comparison between the different channels is shown in Table 7.

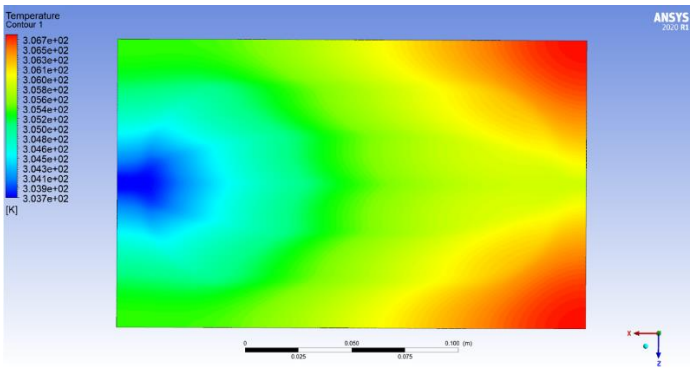

(a)

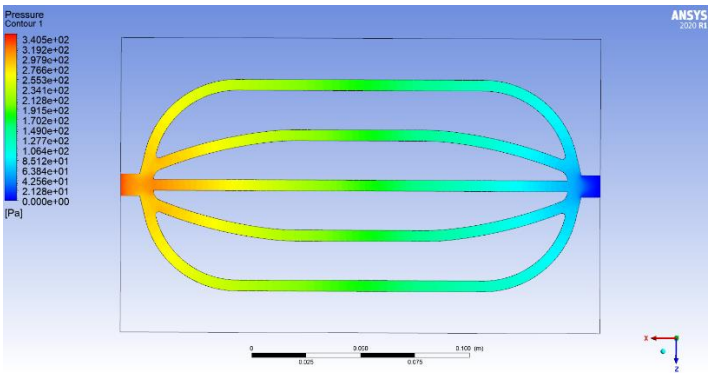

(b)

Figure 18. 5 channels. (a) Temperature distribution. (b) Pressure distribution.

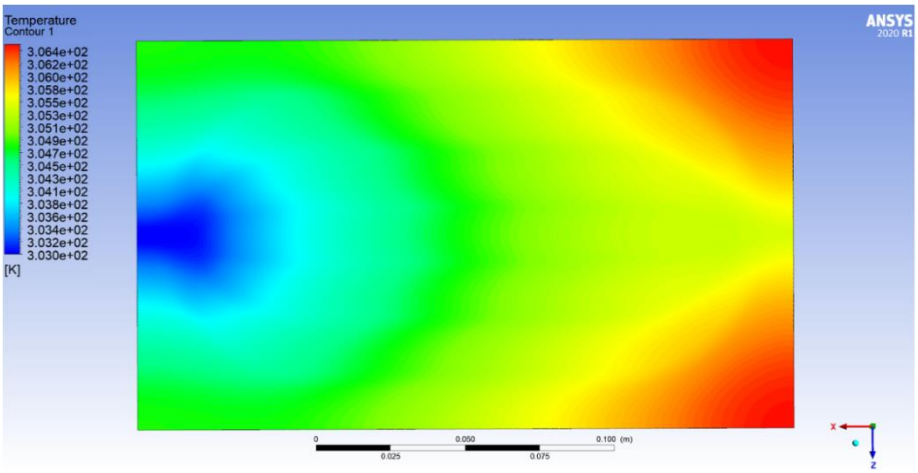

(a)

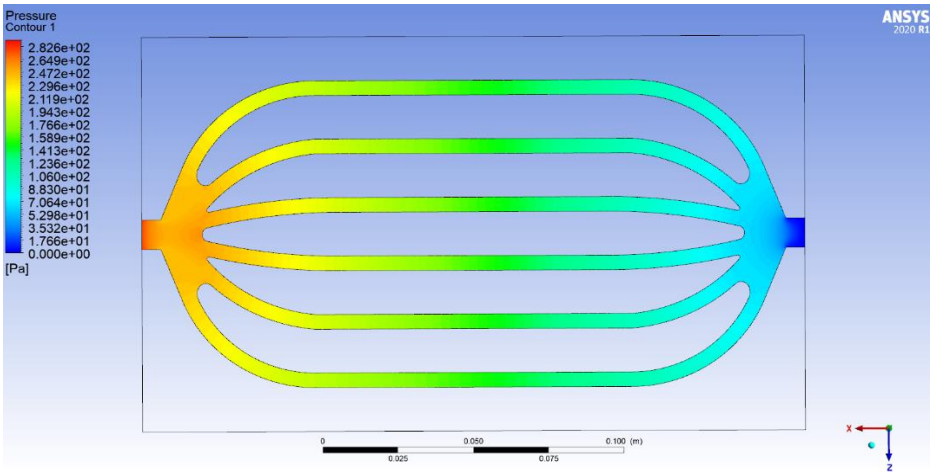

(b)

Figure 19. 6 channels. (a) Temperature distribution. (b) Pressure distribution.

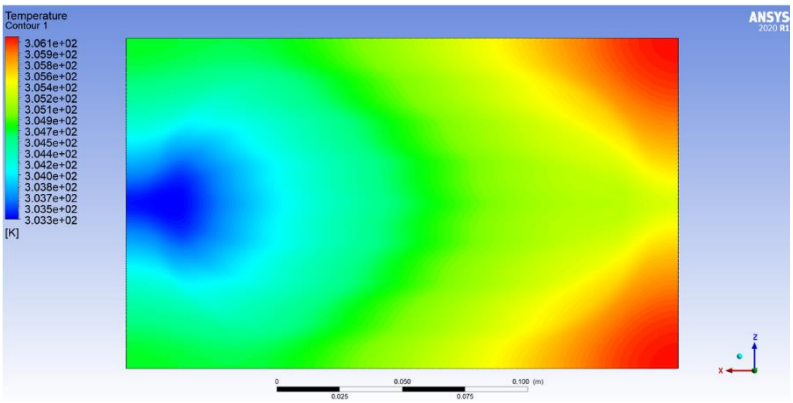

(a)

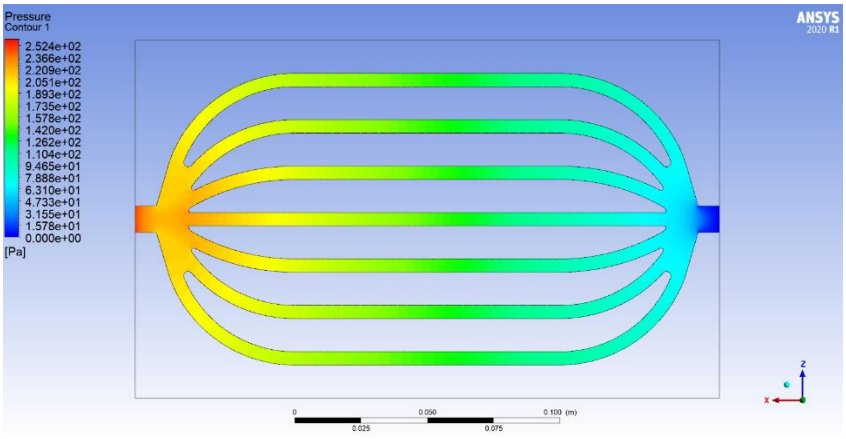

(b)

Figure 20. 7 channels. (a) Temperature distribution. (b) Pressure distribution.

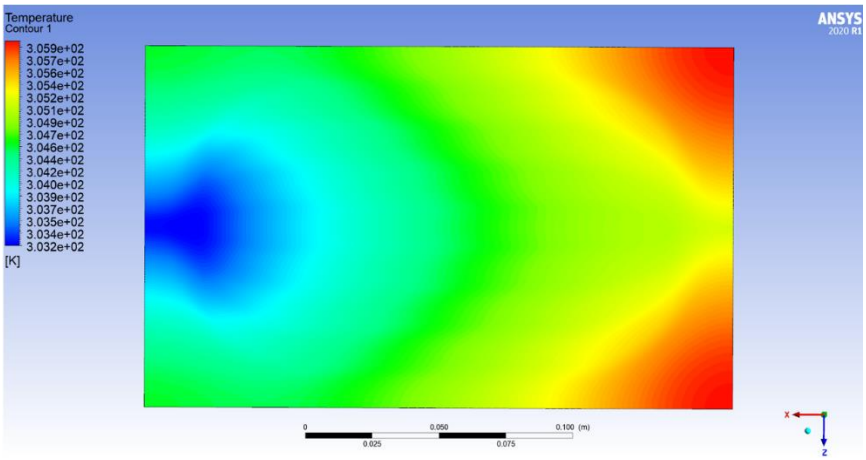

(a)

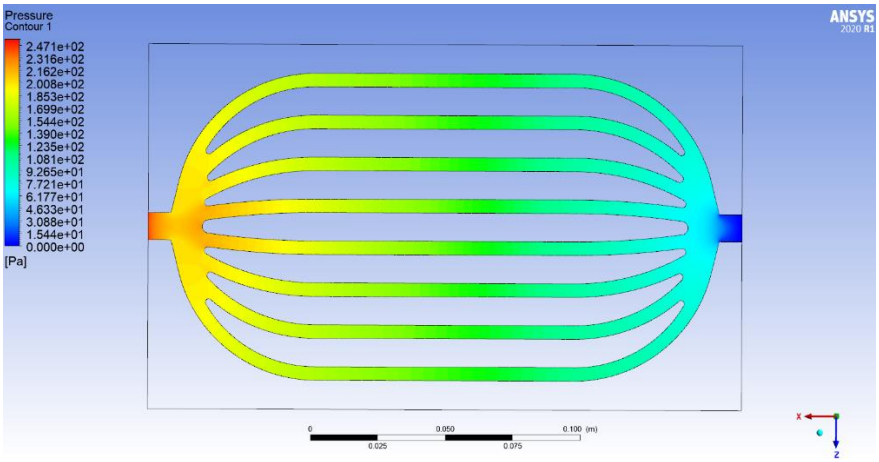

(b)

Figure 21. 8 channels. (a) Temperature distribution. (b) Pressure distribution.

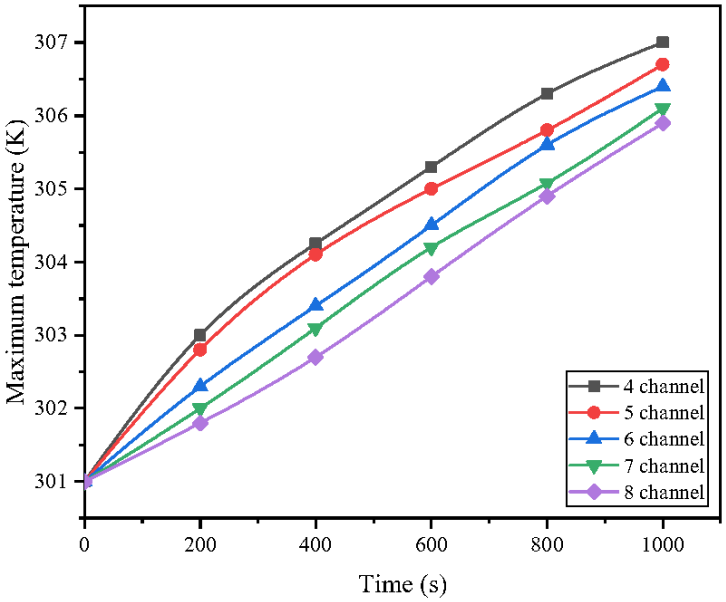

(a)

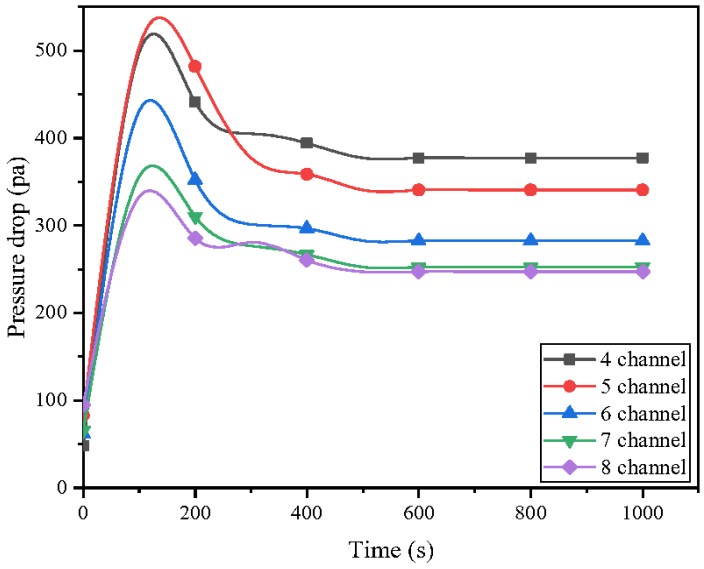

(b)

Figure 22. No. of channels. (a) Temperature gradient. (b) Pressure gradient.

Table 7. Comparison of different channels.

Channels	Max. Temperature (K)	Max. Temperature Difference (K)	Pressure Drop (Pa)
4	307	3.15	377.16
5	306.7	2.97	340.5
6	306.4	3.4	282.628
7	306.1	2.8	252.436
8	305.9	2.67	247.119

Based on the temperature gradient, it is evident that the entrance zone has the lowest temperature, while the output region experiences the highest temperature. As the coolant moves through the channel, this feature indicates that it is continuously absorbing heat. Each model's temperature rise is depicted in multiple channels in this graphic. In the 298K–318K range, Li-ion batteries perform optimally. On a 5-channel plate, the highest temperature that was obtained was 306.7 K, which is sufficient. Temperature gradually drops with increasing channel count. The explanation for this is that when the flow area grows, there is a greater transfer of heat between the coolant and the plate. In addition, the number of channels cannot be increased due to the limitation of the cold plate size. As the number of channels increases, the pressure drop also decreases the percentage reduction is 34.48% from 4 to 8 channel and the percentage reduction in temperature from is approximately 3.25%. The Table 7. shows the lowest temperature, temperature difference and pressure drop of an 8-channel cold plate.

4. Conclusion

In this research, a comprehensive CFD analysis was conducted on the indirect liquid cooling system for electric vehicle (EV) batteries using a cold plate. The study focused on three critical parameters: the effect of different coolants, the impact of various cold plate structures, and the influence of the number of channels.

1. The analysis revealed that water as a coolant result in the lowest surface temperature (307.91 K) and a relatively high temperature difference (4.91 K), indicating a high uniform temperature distribution. In contrast, a 50% ethylene glycol-water (EGW) solution was found to offer better performance by improving corrosion resistance, raising the boiling point, and reducing the freezing point, making it suitable for various operating conditions. Thus, the 50% EGW solution was chosen for further studies.
2. Three different cold plate structures i.e., serpentine, streamline, and straight channels were analyzed. The streamline channel cold plate demonstrated superior performance with the lowest maximum temperature (307 K), the smallest maximum temperature difference (3.15 K), and the least pressure drop (377.16 Pa). Compared to the serpentine channel, the pressure drop in the streamline channel was reduced by 92.17%, and it also showed a temperature decrease of 3.42% compared to the straight channel. These results indicate that the streamline channel cold plate ensures better temperature uniformity and lower pressure drops, making it the most efficient design.
3. The study also examined the effect of varying the number of channels (5, 6, 7, and 8) on the cold plate's performance. Across these configurations, the streamline channel consistently outperformed other structures in terms of maximum temperature, temperature uniformity, and pressure drop. The streamlined design facilitated efficient heat transfer and minimized pressure losses, reaffirming its suitability for EV battery cooling applications.

This research highlights the critical role of coolant selection, structural design, and channel configuration in optimizing the performance of indirect liquid cooling systems for EV batteries. The 50% EGW solution combined with a streamline channel cold plate structure provides the best overall performance, ensuring efficient thermal management and uniform temperature distribution while minimizing pressure drop.

Declaration of competing interest: The authors declare that they have no known competing financial interests or personal relationships that could have appeared to influence the work reported in this paper.

Conflict of interest: The authors declare that they have no conflict of interest.

Funding: There is no funding provided by any Institutions/organizations/funding agencies for this research work.

Data availability statement: The authors declare that the data supporting the findings of this study are available within the paper.

References

[1] Zhao, C.; Zhang, B.; Zheng, Y.; Huang, S.; Yan, T.; Liu, X. Hybrid Battery Thermal Management System in Electrical Vehicles: A Review. *Energies 2020, 13, 6257.* 6257; Doi: https://doi.org/10.3390/en13236257

[2] Aneke, M.; Wang, M. Energy storage technologies and real life applications-A state of the art review. *Appl. Energy 2016, 179, 350–377*; Doi: http://dx.doi.org/10.1016/j.apenergy.2016.06.097

[3] Liu, J.; Chen, H.; Huang, S.; Jiao, Y.; Chen, M. Recent Progress and Prospects in Liquid Cooling Thermal Management System for Lithium-Ion Batteries. *Batteries 2023, 9, 400*; Doi: https://doi.org/10.3390/batteries9080400

[4] Wang, Q.; Jiang, B.; Li, B.; Yan, Y. A critical review of thermal management models and solutions of lithium-ion batteries for the development of pure electric vehicles. Renew. Sustain. *Energy Rev. 2016, 64, 106–128*; Doi: http://dx.doi.org/10.1016/j.rser.2016.05.033

[5] Kim, J.; Oh, J.; Lee, H. Review on battery thermal management system for electric vehicles. *Appl. Therm. Eng. 2019, 149, 192–212*; Doi: https://doi.org/10.1016/j.applthermaleng.2018.12.020

[6] Sourav Singh Katoch and M Eswaramoorthy 2020 *IOP Conf. Ser.: Mater. Sci. Eng. 912 042005*; Doi: https://doi.org/10.1088/1757-899X/912/4/042005

[7] Xu, J.; Zhou, T.; Experimental investigation on a novel cooling device for a prismatic Li-ion battery module operating at high ambient temperature. Sci China Tech sci, 2020, 63. Doi; https://doi.org/10.1007/s11431-020-1605-5

[8] Wang, T.; Zhang, X.; Zeng, Q.; Gao, K. Thermal management performance of cavity cold plates for pouch Li-ion batteries using in electric vehicles. *Energy Sci Eng. 2020; 8:4082–409*; Doi: https://doi.org/10.1002/ese3.798

[9] Aldosry, A.M.; Zulkifli, R.; Wan Ghopa, W.A. Heat Transfer Enhancement of Liquid Cooled Copper Plate with Oblique Fins for Electric Vehicles Battery Thermal Management. *World Electr. Veh. J. 2021, 12, 55*; Doi: https://doi.org/10.3390/wevj12020055

[10] Ye, B.; Haque Rubel, M.R; Li, H. Design and Optimization of Cooling Plate for Battery Module of an Electric Vehicle. *Appl. Sci. 2019, 9, 754*; Doi: https://doi.org/doi:10.3390/app9040754

[11] Huang, Y.; Mei, P.; Lu, Y.; Huang, R.; Yu, X.; Chen, Z.; Roskilly, A.P. A novel approach for Lithium-ion battery thermal management with streamline shape mini channel cooling plates. *Appl. Therm. Eng. 2019, 157, 113623*; Doi: https://doi.org/10.1016/j.applthermaleng.2019.04.033

[12] Wei, L.; Zou, Y.; Cao, F.; Ma, Z.; Lu, Z.; Jin, L. An Optimization Study on the Operating Parameters of Liquid Cold Plate for Battery Thermal Management of Electric Vehicles. *Energies 2022, 15, 9180*; Doi: https://doi.org/10.3390/en15239180

[13] Qian, Z.; Li, Y.; Rao, Z. Thermal performance of lithium-ion battery thermal management system by using mini-channel cooling. *Energy Conversion and Management 126 (2016) 622–631*; Doi: http://dx.doi.org/10.1016/j.enconman.2016.08.063